Journal of Information Systems Engineering and Management
2025, 10(4)
e-ISSN: 2468-4376
https://www.jisem-journal.com/

Research Article

Optimizing Photovoltaic Efficiency in Isolated Areas: A Comparative Study of Fixed and Single-Axis Tracking Systems under Real Climatic Conditions

Louazene Mohammed Lakhdar [1], Bouramdane Abderraouf [2] , Benmir Abdelkader [3]
[1]Laboratory of Electrical Engineering (LAGE) , Department of Electrical Engineering , University of Kasdi Merbah Ouargla , Ouargla 30000 , Algeria .
louazene.lakhdar@univ-ouargla.dz ; bouramdane.abderraouf@univ-ouargla.dz ; ge.abenmir@gmail.com
[2] Department of Electrical Engineering, University Kasdi Merbah Ouargla, Algeria.
*Corresponding author: Louazene Mohammed Lakhdar (e-mail: louazene.lakhdar@univ-ouargla.dz);
Bouramdane Abderraouf (e-mail: bouramdane.abderraouf@univ-ouargla.dz) .

ARTICLE INFO

Received: 08 Jan 2025

Revised: 18 Mar 2025

Accepted: 25 Mar 2025

ABSTRACT

This study presents an experimental simulation aimed at evaluating the performance of four photovoltaic (PV) subfields, each employing two mounting configurations: fixed-tilt and single-axis horizontal tracking systems with an east-west orientation. Two PV technologies, monocrystalline silicon (mc-Si) and polycrystalline silicon (pc-Si), were examined, with each subfield rated at a nominal capacity of 100 kW. All systems were installed at a tilt angle of 30°, optimized for solar energy capture at the experimental site in Ghardaïa, Algeria (32°34'43.79" N, 3°41'55.36" E). The study was conducted over four representative days, corresponding to different seasons.

System performance was evaluated using key indicators, including peak power output (kW), daily average power (KW), and the percentage increase in power based on daily averages(%). The impact of tilt angle and tracking mechanisms on solar energy capture was also assessed. Simulations were carried out using MATLAB-based PV design tools, and power output profiles were generated accordingly. High-resolution measurements recorded at four-minute intervals supported the simulation process and enabled real-time performance tracking.

The results demonstrated that single-axis tracking systems consistently outperformed fixed-tilt configurations, offering enhanced power generation and system efficiency throughout the day. On May 2nd, the mc-Si subfields with fixed and tracking structures achieved peak outputs of 95.96 kW and 92.06 kW, respectively, while the pc-Si equivalents reached 84.93 kW and 83.01 kW. Over the four study days, tracking systems exhibited superior performance in both power production and solar irradiance utilization. Daily average power output were recorded on January 2nd , May 2nd , July 2nd , and October 2nd . The highest average daily power outputs for mc-Si and pc-Si tracking systems were observed on May 2nd, reaching 65.58 kW and 55.96 kW, respectively. Notably, on January 2nd, the tracking systems achieved the highest power gains of 19.30% (mc-Si) and 17.20% (pc-Si) compared to their fixed counterparts, underscoring the advantage of tracking technologies in maximizing daily energy yield.

In parallel, real-time solar irradiance measurements at a 30° tilt angle were obtained using a rooftop-mounted radiometric station. Three empirical models, Perrin de Brichambaut, Liu & Jordan, and Capderou, were assessed for their accuracy in estimating global tilted irradiance. Among them, the Perrin de Brichambaut model yielded the closest agreement with measured values on July 2nd, with a minimum root mean square error (RMSE) of 3.2261 W/m².

Keywords: Photovoltaic systems, Fixed-tilt mounting, Single-axis tracking, Experimental data, Solar irradiance, empirical models, RMSE.

Journal of Information Systems Engineering and Management
2025, 10(4)
e-ISSN: 2468-4376
https://www.jisem-journal.com/

Research Article

I. INTRODUCTION

The rapid growth in global energy consumption driven by industrialization and population increase has historically depended on non-renewable energy sources such as coal, oil, and natural gas. While these sources have supported economic development for decades, their continued use has resulted in serious environmental impacts, including elevated greenhouse gas emissions, global warming, and ecosystem degradation. As a result, there is an urgent need to transition toward cleaner and more sustainable energy alternatives.

Among these, solar energy stands out as one of the most promising options, particularly in regions with high solar potential, such as the Sahara. Numerous studies have confirmed the feasibility of harnessing substantial solar irradiance in these areas under clear-sky conditions (Benatiallah et al., 2017) [1]. Solar radiation supports a wide array of applications, including photovoltaic (PV) power generation, solar desalination, thermal heating, daylighting in buildings, and hydrogen production (Kalogirou, 2004) [2].

Accurate solar radiation assessment is essential for the effective design, modeling, and deployment of photovoltaic systems. Recent techniques, such as the approach developed by Marion and Smith (2017), have shown that solar irradiance components specifically direct normal irradiance (DNI) and diffuse horizontal irradiance (DHI) can be reliably estimated from PV module data equipped with microinverters. This enables more precise project planning across diverse climatic conditions. In addition, several semi-empirical models have been widely applied to estimate global solar radiation on both horizontal and inclined planes. For instance, a relevant case study conducted in Ouargla a region with climatic conditions similar to the Oued-Nechou site in Ghardaïa compared the performance of three well-known models: CAPDEROU, PERRIN DE BRICHAMBAUT, and Hottel. Using data from the LAGE Laboratory at the University of Ouargla, the study found that the CAPDEROU and PERRIN DE BRICHAMBAUT models offered superior accuracy under clear-sky conditions, as evidenced by statistical indicators such as RMSE, correlation coefficient (CC), and MAPE (A. Gougui et al 2018)[4].

In this context, understanding the temporal and spatial characteristics of solar radiation is critical for the design, simulation, and optimization of solar energy systems. It plays a crucial role in evaluating the performance of technologies such as photovoltaic (PV) systems, solar water heaters, concentrating solar power plants, and energy-efficient buildings designed with appropriate thermal insulation. Moreover, solar radiation data particularly direct, diffuse, and global components on an hourly basis is vital for both research and engineering applications. However, the limited availability of high-resolution hourly measurements, especially in regions with complex climatic conditions, presents a challenge to accurately assessing and deploying solar technologies. Therefore, a thorough understanding of solar radiation characteristics is a prerequisite for the successful development and implementation of solar energy solutions.

In Algeria, recent years have witnessed significant governmental initiatives aimed at enhancing solar capacity, particularly in the Saharan regions. As part of its renewable energy strategy, Sonelgaz (The National Gas and Electricity Society) has implemented large-scale PV projects. Notably, in the Oued-Nechou region of Ghardaïa, photovoltaic power plants with a combined production capacity of approximately 1.1 MW have been established. These installations, managed by SKTM (Electricity & Renewable Energy Company), reflect Algeria's growing commitment to clean energy and sustainable development (Sharma and Chandel, 2013 [5]; Dahmoun et al., 2021 [6]). Ensuring that these PV modules operate reliably over a span of 20–25 years under real field conditions is essential for maintaining both energy output and economic viability. According to Dahmoun et al. [6], understanding the performance of photovoltaic systems is a key factor in evaluating the reliability and maintenance requirements of solar installations, in addition to their long-term return on investment. Power production comparisons from international studies further illustrate the importance of system design and location in photovoltaic performance. For example, Shiva Kumar and Sudhakar (2015) [7] analyzed a 10 MWp photovoltaic plant in India, reporting a yield factor (YF) ranging from 1.96 to 5.07 hours/day, an annual performance ratio (PR) of 86.12%, and a capacity factor (CF) of 17.68%, with total annual energy generation reaching 15,798.192 MWh. In a similar vein, Touili et al. (2019) [8] reported that a 100 MWp PV plant in the MENA region achieves an average production of 158 GWh annually. When comparing this to the same configuration installed in different locations, the performance remains remarkably high: 155.8 GWh/year in Almeria, Spain, and 155.4 GWh/year in Bakersfield, California.

Journal of Information Systems Engineering and Management
2025, 10(4)
e-ISSN: 2468-4376
https://www.jisem-journal.com/

Research Article

These results highlight the strong influence of geographical location, solar resource availability, and system configuration including the use of technologies such as solar tracking systems on PV system performance. Tracking systems are particularly important in maximizing the performance of solar panels, as they allow PV modules to continuously align with the sun's path, thereby increasing solar energy capture throughout the day (Touili et al., 2019 [8]).

The motivation for this research arose from a comprehensive review of existing literature focused on photovoltaic (PV) system performance, power generation efficiency, and the prediction of solar energy output. This paper is structured into two main sections, each addressing a critical aspect of photovoltaic system evaluation. The first section centers on the prediction of global solar irradiance on a surface inclined at 30°, utilizing three widely recognized semi-empirical models: PERRIN DE BRICHAMBAUT, LUI & JORDAN, and CAPDEROU. These models were used to estimate irradiance values and were subsequently validated against experimental data recorded at the same tilt angle. The data were obtained from a meteorological station located on the rooftop of the control room at the Ghardaïa photovoltaic power plant. To capture seasonal variability, four representative days were selected January 2nd , May 2nd , July 2nd and October 2nd , in 2016 and. Real-time solar radiation data recorded at 4-minute intervals were employed for the analysis. Model performance was assessed using statistical indicators including the Absolute Error Curve (AE Curve), Mean Absolute Error (MAE), Root Mean Square Error (RMSE), Correlation Coefficient (CC), and Mean Absolute Percentage Error (MAPE). Ghardaïa was selected due to its rich radiometric data and its high potential for solar energy exploitation, making it an ideal site for this study. The second section evaluates the performance of different photovoltaic subfield configurations using key output metrics: peak power (kW), long-term daily power production (kW), average daily output (kW), and the percentage gain in power relative to daily averages (%) , measured over the same four representative days. This part of the study focuses particularly on the performance gains achieved by implementing single-axis tracking systems compared to conventional fixed PV systems. The analysis highlights how solar tracking improves solar radiation capture and, consequently, power generation efficiency throughout the day and across seasons.

II. GEOGRAPHICAL AND METEOROLOGICAL CHARACTERIZATION OF A PHOTOVOLTAIC SITE IN GHARDAÏA

The Ghardaïa photovoltaic solar power plant, located in southern Algeria, is part of the national renewable energy development program initiated by the relevant ministry. It is situated near the village of Oued-Nechou, approximately 15 km north of Ghardaïa along National Road No. 01, with a nominal installed capacity of around 1,100 kWp. The site is bordered by National Road No. 01 to the north and west, while undeveloped land lies to the east and south. Geographically, the plant is positioned at a latitude of 32°34'43.79" N and a longitude of 3°41'55.36" E, at an elevation ranging from 450 to 566 meters above sea level. The nearest neighboring wilayas are Laghouat and Ouargla, and the topography of the site is relatively flat, with a slight gradient from east to west.

In terms of climate, the region of Ghardaïa is characterized by hot and arid conditions that present extreme environmental challenges. Temperatures range from -5°C to +50°C in the shade, and wind speeds can reach up to 28 m/s. The highest recorded relative humidity is 74% at 25°C. During the summer, solar irradiance levels typically range between 900 and 1000 W/m². Additionally, the region experiences significant diurnal temperature variations of 15 to 20°C and frequent winds that carry fine sand particles. These factors are crucial to consider for the design, operation, and maintenance of photovoltaic systems. Despite these constraints, the plant is located in seismic zone 0, which indicates a low seismic risk according to Algerian seismic regulations (RPA 99).

The geographical location of the Oued Nechou photovoltaic power plant, situated in the Ghardaïa region of southern Algeria, is illustrated in Fig I.

Journal of Information Systems Engineering and Management
2025, 10(4)
e-ISSN: 2468-4376
https://www.jisem-journal.com/

Research Article

Fig 1. Geographical location of the photovoltaic power plants: 1.1 MWp OUED-NECHOU, Ghardaïa City [9] .

II. METEOROLOGICAL STATION INSTALLED AT THE PHOTOVOLTAIC PLANT IN OUED-NECHOU, GHARDAÏA CITY

The photovoltaic power plant located in Oued-Neachou , Ghardaïa, features a meteorological station installed on the roof of the control room. This station is used to gather meteorological data and primarily consists of:

Fig 2 . Metrology Station of Solar PV Panels Center Oued-Nechou, Ghardaïa.

a) Barometer to measure atmospheric pressure.

b) Rain gauge to measure the amount of rain.

c) Humidity measurement.

d) Wind speed measurement.

e) Wind direction measurement.

f) Pyranometers to measure direct, diffuse and inclined radiation.

g) Ambient temperature sensor.

h) Instrument for measuring the duration of sunshine.

Journal of Information Systems Engineering and Management
2025, 10(4)
e-ISSN: 2468-4376
https://www.jisem-journal.com/

Research Article

III. EMPIRICAL ESTIMATION OF HOURLY SOLAR RADIATION

Due to the limited number of meteorological stations across the national territory, empirical models are frequently employed to estimate solar irradiation. These models rely on theoretical correlations to extend their applicability to locations lacking direct solar radiation measurements [1-17].

To accurately determine the solar radiation received by a surface at a given location, both direct and diffuse components must be measured or estimated. In the absence of direct observational data, empirical models are used to estimate these components. Consequently, several well-known models have been developed for estimating global, direct, and diffuse solar radiation, including those proposed by Michel Capderou, Perrin de Brichambaut, R. Sun, Liu & Jordan, Atwater & Ball, and Bird & Hulstrom.

In this study, three widely used empirical models are selected for comparison: the Liu & Jordan model, the Capderou model (both incorporating the Linke turbidity factor), and the Perrin de Brichambaut model. These models are applied to estimate global solar radiation on an inclined surface and are validated against experimental data obtained from the meteorological station at the SKTM Center in the Oued-Nechou region. Data collection was conducted on four representative days in 2016, each corresponding to a different season: January 2nd (Winter), May 2nd (Spring), July 2nd (Summer), and October 2nd (Autumn).

The analysis is performed using a 30° tilt angle, which closely approximates the optimal inclination for maximizing solar energy capture throughout the year in the Ghardaïa region. To assess the reliability of the selected models, statistical evaluation methods are applied to determine which model most accurately reflects the measured data. The most accurate model is then recommended for solar radiation studies in areas where direct meteorological data are unavailable.

The tilt angle of a surface plays a significant role in the amount of solar radiation it receives. Adjusting this angle allows for an optimal combination of direct, diffuse, and ground-reflected radiation, thereby maximizing total solar energy collection.

The global solar irradiance on an inclined surface (denoted asH_T) consists of three main components: direct beam radiation (H_B), diffuse radiation (H_D), and ground-reflected radiation (H_R). Under the assumption of isotropic reflection, the total irradiance can be calculated using the equation proposed by Duffie and Beckman (1991) [17], [18].

$$H_T = H_B + H_D + H_R \quad (1)$$

III.1. Linke Turbidity Factor

Understanding the atmospheric turbidity factor is essential for accurately estimating solar irradiance under clear sky conditions. The Linke turbidity factor (T_L) quantifies the attenuation of solar radiation due to atmospheric constituents such as water vapor, aerosols, and dust. Specifically, it represents the number of clean, dry atmospheres that would produce the same level of attenuation as the actual atmosphere at a given location. This factor integrates several atmospheric effects into a single parameter, offering a practical means to characterize solar radiation in varying atmospheric conditions **[4],[19].**

$$T_L = T_0 + T_1 + T_2 \quad (2)$$

T_0 **:** representing the gaseous absorption component of turbidity, is estimated using Capderou's geo-astronomical model as follows:

$$T_0 = 2.4-0.9\times\sin(\Phi)+ 0.1 \times (2+\sin(\Phi)) \times Ahe -0.2 \times Z - (1.22+0.14\times Ahe) \times (1-\sin(h)) \quad (3)$$

$$Ahe = \sin\left[\left(\frac{360}{365}\right) \times (n-121)\right] \quad (4)$$

Z: altitude de lieu [Km].

T_1**:** represents the turbidity due to absorption by atmospheric gases (O_2, CO_2, and O_3), as well as molecular Rayleigh scattering. This component is modeled according to the formulation provided in **[19]**.

$$T1 = 0.89^{Z} \quad (5)$$

Journal of Information Systems Engineering and Management
2025, 10(4)
e-ISSN: 2468-4376
https://www.jisem-journal.com/

Research Article

T_2: accounts for the turbidity caused by aerosol scattering, along with minor absorption effects. It varies depending on both the type and concentration of aerosols present in the atmosphere**[4],[16],[19-20].**

$$T2 = (0.9+0.4 \times Ahe) \times (0.63)^{Z} \quad (6)$$

III.2 . LUI & JORDAN Model

III.2.1- Solar radiation formulas on an inclined plane : The Liu and Jordan model provides a widely used empirical method for estimating global solar irradiance on a tilted surface. In this model, the global radiation on an inclined plane is composed of three components: direct radiation, isotropic diffuse radiation, and diffuse radiation from the sky, as given by the following equation , For more detailed scientific background, the original sources provide comprehensive explanations**.[14],[16]**

$$G_T = S_H \times R_b + D_H \times \left(\frac{1+cos(\beta)}{2}\right) + (S_H + D_H) \times \left(\frac{1-\cos\beta}{2}\right) \times \rho \quad (7)$$

III.3. PERRIN DE BRICHAMBAUT Model

The empirical model developed by Perrin de Brichambaut is based on extensive experimental measurements conducted at the Trappes center (Paris region) and in Carpentras (southern France). This model has demonstrated applicability across various global regions, with the exception of areas experiencing high atmospheric dust concentrations such as the Sahel, including countries like Mali and Niger particularly during specific periods of the year. In the context of Algeria, experimental studies have confirmed the reliability of the Perrin de Brichambaut formulas in both the northern and southern parts of the country **[14],[15].**

III.3.1 Solar radiation on an inclined plane in the Perrin model

This empirical equation below represents total irradiance as the sum of physical components. Further details are available in the referenced studies **[4],[14],[16],[19]**.

$$G_T = S + D_{ciel} + D_{sol} \quad (8)$$

III.4. CAPDEROU Model

The Capderou model **[21]**, **[22]** is founded on the concept of atmospheric turbidity factors, which quantify the absorption and scattering effects of atmospheric constituents. These factors allow for the calculation of direct and diffuse solar irradiance under clear sky conditions, both on horizontal and inclined surfaces. Accurate knowledge of the atmospheric turbidity factor is crucial for estimating global irradiance in clear sky scenarios

IIII.4.1. Global illumination received on an inclined surface according to the CAPDEROU model

See references **[4],[16]** for further details on the model and its components

$$I = I_0 \times C_{ts} \times exp\left[-T_L \left(0.9 + \frac{9.4}{0.89^{Z}} \times \sin(h)\right)^{-1}\right] \times cos(i) \quad (9)$$

IV. SOFTWARE TOOLS

The dynamic system modeling was performed using MATLAB (MathWorks R2021b), an interactive platform that provides a comprehensive suite of tools for developing hourly solar radiation models. MATLAB's environment enables the rapid construction of detailed block diagrams, facilitating efficient system simulation.

By integrating geographical coordinates, the number of days in the year, and atmospheric data, the software calculates the global solar radiation on an inclined surface at the Oued Nechou site in Ghardaïa. This is achieved through the implementation of the Perrin de Brichambaut, Liu & Jordan, and Capderou models within MATLAB (MathWorks R2021b). Two distinct models were executed, and for each evaluation day, corresponding graphs were generated showing both the total daily radiation and the absolute error curves, enabling a thorough comparative analysis.

V. RESULTS AND INTERPRETATION

Journal of Information Systems Engineering and Management
2025, 10(4)
e-ISSN: 2468-4376
https://www.jisem-journal.com/

Research Article

Irradiance measurements were conducted at the OUED-NECHOU photovoltaic power plant in central Ghardaïa using a pyranometer, which generates a voltage proportional to solar irradiance (in W/m²). These measurements enable an accurate evaluation of solar radiation incident on the 30°-tilted PV panels installed at the site.

Three solar radiation models, PERRIN DE BRICHAMBAUT, LUI & JORDEN, and CAPDEROU, were compared against the experimental data to assess the accuracy of various estimation models. Simulations were carried out in MATLAB on four representative days in 2016: January 2nd , May 2nd , July 2nd , and October 2nd , each corresponding to a different season.

Solar radiation data were recorded at 4-minute intervals from 06:00 AM to 08:00 PM. The following figures present comparative plots of the global irradiance on the inclined surface, simulated by the three models and validated against the pyranometer measurements. Each curve is color-coded to distinguish between experimental and estimated data, and an additional curve illustrates the absolute error, as presented in Figures 3, 4, 5, and 6.

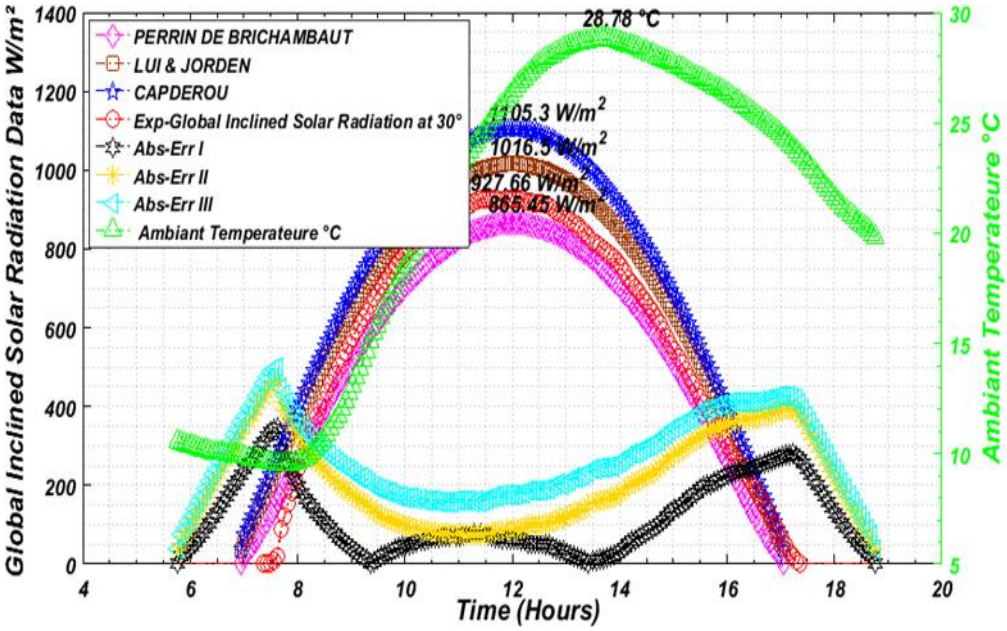

Fig. 3. Comparison of Simulated and Measured Inclined Solar Radiation on January 2nd , 2016 (Winter Day).

Figure 3 compares global inclined solar radiation estimates from three empirical models, PERRIN DE BRICHAMBAUT, LUI & JORDEN, and CAPDEROU, with experimental data recorded on January 2nd , a typical winter day. The analysis covers the period from sunrise to sunset and includes absolute error curves to evaluate model accuracy.

The measured solar irradiance peaked at 865.45 W/m². Among the models, PERRIN DE BRICHAMBAUT predicted 927.66 W/m², LUI & JORDEN 1016.5 W/m², and CAPDEROU 1105.3 W/m². PERRIN DE BRICHAMBAUT provided the closest approximation, particularly during the morning and late afternoon. LUI & JORDEN, and CAPDEROU consistently overestimated values, with CAPDEROU showing the most significant deviation and lowest accuracy. The ambient temperature peaked smoothly at 28.78°C, correlating clearly with radiation intensity.

Error analysis shows PERRIN DE BRICHAMBAUT maintains low error except for a slight rise near noon. LUI & JORDEN's error grows as radiation increases, while CAPDEROU exhibits the highest errors at peak irradiance, confirming its poorer performance.

Journal of Information Systems Engineering and Management
2025, 10(4)
e-ISSN: 2468-4376
https://www.jisem-journal.com/

Research Article

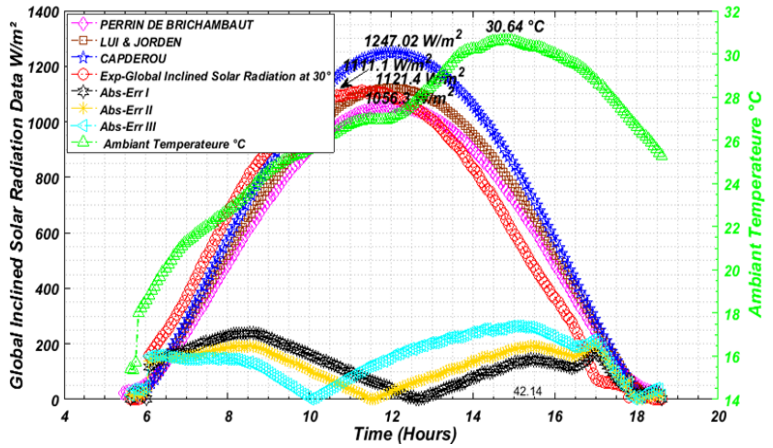

Fig. 4 . Comparison of Inclined Solar Radiation Estimates from Three Models with Experimental Data on May 2nd , 2016, Spring Day

Figure 4 presents a comparative assessment of three empirical models, PERRIN DE BRICHAMBAUT, LUI & JORDEN, and CAPDEROU, against experimental data for global inclined solar radiation at 30°. The analysis, conducted on May 2nd (spring season), spans the whole daylight period and records a peak ambient temperature of 30.64°C.

The experimental curve displays a smooth increase from sunrise, peaking at 1111.1 W/m² around midday. Among the models, CAPDEROU significantly overestimates the irradiance, reaching a maximum of 1247.02 W/m². LUI & JORDEN provide the closest estimate to the measured value, with a peak of 1121.4 W/m², showing a minimal deviation of 10.3 W/m². In contrast, PERRIN DE BRICHAMBAUT predicts the lowest peak at 1056.3 W/m², underestimating the observed maximum. Although all models generally follow the experimental trend, deviations are most pronounced around solar noon. The ambient temperature shows a steady increase, reaching its maximum concurrently with the solar radiation peak. This synchronization highlights the strong correlation between ambient temperature and solar irradiance throughout the day.

The absolute error analysis further supports these findings. LUI & JORDEN'S model exhibits the lowest peak error, confirming its superior accuracy in estimating maximum irradiance. While CAPDEROU captures the overall trend, it tends to overpredict irradiance values. PERRIN DE BRICHAMBAUT, though consistently underestimating, maintains a relatively stable error profile throughout the day. Overall, LUI & JORDEN demonstrate the best agreement with the experimental data, making it the most reliable model for this dataset.

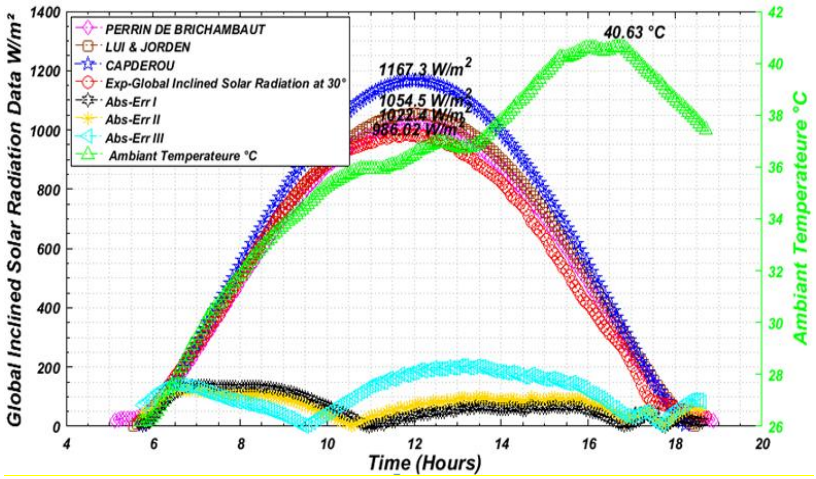

Fig 5. Comparison of Inclined Solar Radiation Estimates from Three Models with Experimental Data on July 2nd, 2016 A Summer Day.

Journal of Information Systems Engineering and Management
2025, 10(4)
e-ISSN: 2468-4376
https://www.jisem-journal.com/

Research Article

Fig 5 illustrates a comparative analysis of three empirical models, PERRIN DE BRICHAMBAUT, LUI & JORDEN, and Capderou, against experimental measurements of global inclined solar radiation at a 30° tilt, recorded on July 2nd, a representative summer day. The dataset spans the full diurnal cycle from sunrise to sunset, capturing the temporal evolution of solar irradiance and ambient temperature throughout the day.

The experimental curve shows a smooth increase in irradiance from sunrise, peaking at 986.02 W/m² around midday before declining steadily toward sunset. Among the models, Capderou significantly overestimates the peak with 1167.3 W/m², followed by LUI & JORDEN at 1054.5 W/m², both exceeding the measured values. Perrin de Brichambaut, with a peak of 1022.4 W/m², provides the closest approximation, making it the most accurate in this scenario.

The absolute error curves support this observation. PERRIN DE BRICHAMBAUT consistently exhibits the lowest deviation throughout the day, particularly during peak irradiance hours. LUI & JORDEN present moderate error levels, while CAPDEROU records the highest discrepancies due to its tendency to overestimate radiation levels across most of the daylight period.

The ambient temperature increases steadily in the morning, reaching a maximum of 40.63 °C in the early afternoon. This temperature trend aligns with the irradiance peak and underscores the thermal impact on PV systems, where elevated temperatures may reduce conversion efficiency. In conclusion, for July 2nd conditions, PERRIN DE BRICHAMBAUT proves to be the most reliable model, demonstrating the best alignment with experimental data and minimal error, while LUI & JORDEN and CAPDEROU show more pronounced deviations.

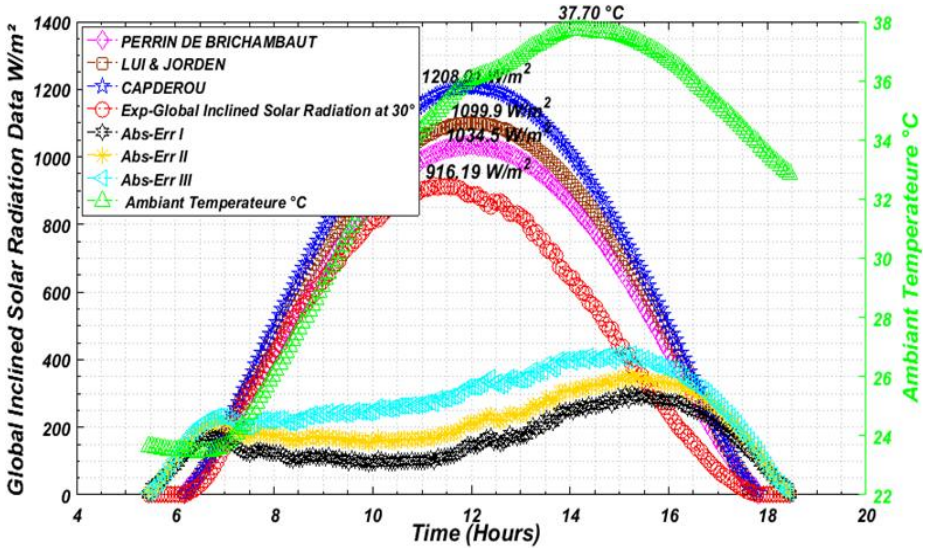

Fig 6. Comparison of Inclined Solar Radiation Estimates from Three Empirical Models with Experimental Data on October 2nd, 2016 - A Fall Day.

Figure 6 presents a detailed evaluation of the accuracy of three empirical models, PERRIN DE BRICHAMBAUT, LUI & JORDEN, and CAPDEROU, in simulating global inclined solar radiation at 30° on October 2nd. This high-temperature autumn day, with a peak ambient temperature of 42.14 °C, serves as a benchmark for assessing model performance over the entire diurnal cycle.

Among the models, PERRIN DE BRICHAMBAUT shows the closest alignment with the experimental curve, peaking at 1034.5 W/m². Its moderate overestimation and consistently low deviation throughout the day confirm its strong predictive accuracy. LUI & JORDEN share a similar peak value but show slightly larger deviations during peak hours. CAPDEROU significantly overestimates the maximum, reaching 1208.01 W/m², representing the most significant discrepancy from the measured data.

The absolute error curves reinforce these findings. PERRIN DE BRICHAMBAUT maintains the lowest error across most of the day, particularly during midday, while Capderou consistently yields the highest errors.

Journal of Information Systems Engineering and Management
2025, 10(4)
e-ISSN: 2468-4376
https://www.jisem-journal.com/

Research Article

Ambient temperature rises steadily in the morning, peaking at 37.70 °C in the early afternoon before declining. This thermal profile directly impacts PV performance, as elevated temperatures increase thermal losses and reduce energy conversion efficiency.

In summary, Perrin de Brichambaut proved to be the most reliable model, closely matching the experimental data with the lowest overall errors. LUI & JORDEN followed with moderate deviations, while CAPDEROU significantly overestimated radiation levels. These results highlight PERRIN DE BRICHAMBAUT as the most suitable model for these conditions, especially under high ambient temperatures, which can negatively affect PV system efficiency.

VI. MODELS EVALUATION

Four statistical indicators were used to evaluate the accuracy of the solar radiation models against experimental data AE Curve **[14]** Mean Absolute Error (MAE) W/m² **[4],[14-16]** , Root Mean Square Error (RMSE) W/m² **[4],[14-16]**, Mean Absolute Percentage Error (MAPE) % **[4],[14-16]**, and the Coefficient of Determination (CC) **[4],[14-16]**. These metrics quantify both the magnitude and distribution of errors between estimated and measured values.

MAE (W/m²) and RMSE (W/m²) assess average and squared deviations, with RMSE giving more weight to larger errors. MAPE (%) provides a percentage-based error, offering a scale-independent comparison. CC reflects the proportion of variance in the measured data explained by the model. Together, these indicators form a robust framework for comparing model performance. Tables below presents the statistical results obtained across the four experimental days **[23-27] .**

Table II : Statistical Test Results of the Three Empirical Models on January 2nd , 2016 .

Day	Empirical models	MAE (W/m²)	RMSE (W/m2)	MAPE (%)	CC
January 2nd ,2016	Perrin De Brichambaut	**97.0995**	**7.3320**	**1.1240**	**0.9963**
	Lui & Jorden	**103.5828**	**10.7183**	**2.1323**	**0.9332**
	Capderou	**153.2530**	**17.6439**	**4.325**	**0.9521**

Table III : Statistical Test Results of the Three Empirical Models on May 2nd , 2016

Day	Empirical models	MAE (W/m²)	RMSE (W/m2)	MAPE (%)	CC
May 2nd .2016	Perrin De Brichambaut	**55.5830**	**4.2737**	**0.8925**	**0.9112**
	Lui & Jorden	**66.2512**	**5.0293**	**1.2256**	**0.9366**
	Capderou	**89.3325**	**11.2523**	**1.7855**	**0.9255**

Table IV : Statistical Test Results of the Three Empirical Models on July 2nd , 2016

Day	Empirical models	MAE (W/m²)	RMSE (W/m2)	MAPE (%)	CC
July2nd ,2016	Perrin De Brichambaut	**76.2552**	**3.2261**	**3.3321**	**0.9965**
	Lui & Jorden	**77.3393**	**6.4132**	**11.251**	**0.9888**
	Capderou	**88.6321**	**10.225**	**21.225**	**0.9443**

Journal of Information Systems Engineering and Management
2025, 10(4)
e-ISSN: 2468-4376
https://www.jisem-journal.com/

Research Article

Table V: Statistical Test Results of the Three Empirical Models on October 2nd , 2016.

Day	Empirical models	MAE (W/m²)	RMSE (W/m2)	MAPE (%)	CC
October 2nd ,2016	Perrin De Brichambaut	**101.2542**	**6.3258**	**2.6544**	**0.9885**
	Lui & Jorden	**152.336**	**8.2236**	**5.1248**	**0.8993**
	Capderou	**155.25**	**10.2547**	**7.2143**	**0.8812**

- On January 2nd , 2016, Table II shows that PERRIN DE BRICHAMBAUT outperformed the other models across all statistical indicators. It recorded the lowest MAE (97.10 W/m²), RMSE (7.33 W/m²), and MAPE (1.12%), indicating the highest accuracy and least deviation from observed values. In contrast, CAPDEROU had the highest errors (MAE: 153.25 W/m²; RMSE: 17.64 W/m²; MAPE: 4.33%), making it the least accurate. LUI & JORDEN showed intermediate performance. Regarding correlation with observed data, all models demonstrated strong agreement, with Perrin de Brichambaut achieving the highest correlation coefficient (CC = 0.9965).
- On May 2nd , 2016, Table III presents the evaluation of three empirical models, PERRIN DE BRICHAMBAUT, LUI & JORDEN, and CAPDEROU based on statistical indicators: Mean Absolute Error (MAE), Root Mean Square Error (RMSE), Mean Absolute Percentage Error (MAPE), and Correlation Coefficient (CC). PERRIN DE BRICHAMBAUT yielded the most accurate results, with the lowest MAE (55.5830 W/m²), RMSE (4.2737 W/m²), and MAPE (0.8925%), indicating minimal deviation from observed values. LUI & JORDEN followed with an MAE of 66.2512 W/m², RMSE of 5.0293 W/m², and MAPE of 1.2256%. CAPDEROU showed the least accuracy, recording the highest MAE (89.3325 W/m²), RMSE (11.2523 W/m²), and MAPE (1.7855%). In terms of correlation, LUI & JORDEN achieved the highest CC at 0.9366, slightly outperforming CAPDEROU (0.9255) and PERRIN DE BRICHAMBAUT (0.9112). Despite this, all models demonstrated a strong correlation with observed data.
- On July 2nd , 2016, Table IV presents a statistical evaluation of three empirical models: PERRIN DE BRICHAMBAUT, LUI & JORDEN, and CAPDEROU. Among them, PERRIN DE BRICHAMBAUT achieved the best overall accuracy, with the lowest MAE (76.2552 W/m²), RMSE (3.2261 W/m²), and MAPE (3.3321%), along with the highest Correlation Coefficient (CC) of 0.9965, indicating a strong alignment between predicted and observed values. LUI & JORDEN showed moderate performance, recording an MAE of 77.3393 W/m², RMSE of 6.4132 W/m², and MAPE of 11.251%, with a CC of 0.9888. CAPDEROU yielded the least accurate results, with the highest MAE (88.6321 W/m²), RMSE (10.225 W/m²), and MAPE (21.225%). Its CC of 0.9443 reflects the weakest correlation among the three models.
- On October 2nd , 2016, Table V presents a statistical comparison of the three empirical models. PERRIN DE BRICHAMBAUT demonstrated the highest accuracy, with the lowest MAE (101.2542 W/m²), RMSE (6.3258 W/m²), and MAPE (2.6544%), along with a strong Correlation Coefficient (CC) of 0.9885. LUI & JORDEN showed moderate performance, with higher error values (MAE = 152.336 W/m², RMSE = 8.2236 W/m², MAPE = 5.1248%) and a lower CC of 0.8993. CAPDEROU had the weakest results, recording the highest errors (MAE = 155.25 W/m², RMSE = 10.2547 W/m², MAPE = 7.2143%) and the lowest CC (0.9012), indicating less reliability in prediction.
- In conclusion, an analysis of the statistical indicators Mean Absolute Error (MAE), Root Mean Square Error (RMSE), Mean Absolute Percentage Error (MAPE), and Correlation Coefficient (CC) across the experimental days of January 2nd, May 2nd, July 2nd, and October 2nd demonstrates that the PERRIN DE BRICHAMBAUT model consistently provides the best alignment with the experimental data .

Journal of Information Systems Engineering and Management
2025, 10(4)
e-ISSN: 2468-4376
https://www.jisem-journal.com/

Research Article

VII. OVERVIEW OF THE PHOTOVOLTAIC SYSTEM AT THE OUED-NECHOU SOLAR POWER PLANT IN GHARDAÏA

The Ghardaïa photovoltaic solar power plant, developed by the Algerian Electricity Production Company (SPE), is located about 15 km north of Ghardaïa, near the village of OUED-NECHOU. Covering an area of ten hectares, the plant converts sunlight directly into electricity, supporting Algeria's renewable energy goals.

With a nominal capacity of approximately 1100 kWp, this pilot project evaluates the performance of various photovoltaic (PV) technologies under the harsh climatic conditions of southern Algeria, characterized by high solar radiation and temperature fluctuations. The facility comprises eight subfields, each featuring four distinct PV module technologies installed on two types of mounting structures: fixed and motorized. The modules are oriented south with a tilt angle of 30° to maximize solar energy capture.

Figure 7 illustrates the PV accessory center at OUED-NECHOU, showcasing the main solar technologies deployed. This pilot plant is instrumental in assessing the technical performance and economic viability of different PV systems in desert conditions, providing valuable insights for future large-scale photovoltaic projects across southern Algeria.

Fig 7. Photovoltaic Installation of OUED-NECHOU, Ghardaïa.

VIII. DISTRIBUTION AND CONFIGURATION OF PHOTOVOLTAIC TECHNOLOGIES AT THE OUED-NECHOU POWER PLANT

The OUED-NECHOU photovoltaic power plant comprises eight (08) subfields, each utilizing one of four PV technologies: monocrystalline silicon, polycrystalline silicon, cadmium telluride (CdTe), and amorphous silicon. Two types of mounting structures are implemented fixed and single-axis motorized tracking systems with all modules oriented due south and tilted at 30° to optimize solar exposure.

Each technology is deployed across specific subfields, depending on its structural configuration. Monocrystalline and polycrystalline modules are installed on both fixed and tracking systems, with 30% mounted on motorized supports and 70% on fixed structures. The total installed capacity for monocrystalline silicon is 465 kWp, distributed across Subfields 1 (105 kWp, tracking), 5 (105 kWp, fixed), and 7 (255 kWp, fixed). For polycrystalline silicon, the combined capacity is 455.9 kWp, from Subfields 2 (98.7 kWp, tracking), 6 (98.7 kWp, fixed), and 8 (258.5 kWp, fixed).

CdTe and amorphous silicon modules are exclusively installed on fixed structures, reflecting their suitability for stable mounting environments. Their respective installed capacities are 100.8 kWp and 100.116 kWp.

Journal of Information Systems Engineering and Management
2025, 10(4)
e-ISSN: 2468-4376
https://www.jisem-journal.com/

Research Article

The six subfields with power ratings around 100 kWp (Subfields 1 to 6) are each connected to individual PV8L121 inverters (100 kW). These inverters are connected in parallel via a low-voltage (LV) switchboard, and the collected energy is routed to a 30/0.4 kV step-up transformer rated at 750 kVA.

The two larger subfields Subfield 7 (255 kWp) and Subfield 8 (258.5 kWp) are each connected to a PV8M291 inverter (250 kW). These inverters are connected to the secondary windings of a 30/0.27 kV transformer rated at 630 kVA, as shown in the General Single-Line Diagram.

IX. TECHNICAL SPECIFICATIONS OF PHOTOVOLTAIC MODULE TYPES

This simulation-based experiment aims to compare the performance of four photovoltaic subfields using monocrystalline (mc-Si) and polycrystalline (pc-Si) technologies, installed on fixed-tilt and motorized single-axis tracking systems. All subfields are oriented due south at a 30° tilt and designed for a nominal capacity of 100 kW. Figure 8 illustrates the layout of the fixed systems, while Figure 9 shows the single-axis tracking configurations. Detailed technical specifications for each PV technology are provided in Table VI.

IX.1. Design and Configuration of Fixed and Single-Axis Tracking Systems for Photovoltaic Panels

The following figure 8 ,9 illustrates the structural configurations of the photovoltaic subfields, highlighting both fixed-tilt and single-axis tracking systems All mounting structures are inclined at 30°, which closely aligns with the optimal tilt angle. These configurations are designed to optimize solar energy capture based on panel orientation and mounting structure. The layouts are essential for understanding the physical arrangement and operational principles of each PV installation**.**

Fig 8. Fixed-Mount Photovoltaic Configuration for Monocrystalline (mc-Si) and Polycrystalline (pc-Si) Subfields.

Fig 9. Single-Axis Tracking Structure of the Photovoltaic System in the OUED-NECHOU Subfields for Monocrystalline (mc-Si) and Polycrystalline (pc-Si) Technologies

Journal of Information Systems Engineering and Management
2025, 10(4)
e-ISSN: 2468-4376
https://www.jisem-journal.com/

Research Article

IX.2 Photovoltaic Technologies: Key Technical Parameters

Table 4 presents the electrical specifications of the photovoltaic modules under standard test conditions (1000 W/m² irradiance, 25 °C temperature, and AM1.5 spectrum). For both monocrystalline and polycrystalline technologies, the parameters remain consistent across fixed-tilt and single-axis tracking configurations, in accordance with the manufacturer's specifications.

Photovoltaic Technologies	Monocrystalline (mc-Si)	Polycrystalline (pc-Si)
Electrical Characteristics		
Type	SOLARIA S6M-2G	SOLARIA S6P-2G
Peak power	245 Wc	235 Wc
Peak power tolerance	0 / +5 Wc	0 / +5 WC
Module performance	15%	14.4%
Max voltage (Vmpp)	30.33 V	30.49V
Max intensity (Impp)	8.08 A	7.71A
Open circuit voltage	37.82 V	37.62V
Short circuit current	8.52 A	8.40 A
Max system voltage	1000 V	1000V
Reference Standards	IEC 61730-1, IEC 61730-2, IEC 61215	IEC 61730-1, IEC 61730-2, IEC 61215
NOCT (Nominal Operating Cell Temperature)	46 +/- 2 [°C]	46 +/- 2 [°C]
Temperature coefficient Isc	+0,015% [°K]	+0.02% [°K]
Temperature coefficient Voc	- 0,31% [°K]	- 0.29% [°K]
Temperature coefficient Pmax	-0,46% [°K]	-0.43% [°K]
NOCT (Nominal Operating Cell Temperature)	46 +/- 2 [°C]	46 +/- 2 [°C]
Temperature coefficient Isc	+0,015% [°K]	+0.02% [°K]

X. PERFORMANCE EVALUATION AND EXPERIMENTAL COMPARISON METHODS FOR PHOTOVOLTAIC SUBFIELDS

In this experimental section, we evaluate four key parameters related to the performance of photovoltaic (PV) systems. First, we examine the impact of tracking systems compared to fixed structures in terms of solar energy capture and their contribution to enhancing PV system efficiency. Second, we analyze the peak power output (kW), which refers to the maximum power generated during a given day. Third, we assess the long-term daily power production (kWh) to evaluate the system's consistency and reliability over time. Finally, we consider the average daily output, which includes daily power production (KW) and the mean daily gain in power (%). This comprehensive approach provides an overall view of the daily generation capacity of the PV systems under study.

The experimental evaluation at the OUED-NECHOU PV station in a semi-arid Saharan region is based on data from four distinct seasonal days in 2016, offering insights into how weather variations, especially solar radiation, affect PV subfield performance.

Journal of Information Systems Engineering and Management
2025, 10(4)
e-ISSN: 2468-4376
https://www.jisem-journal.com/

Research Article

X.1. Solar Irradiance Data Analysis

Climatic, environmental, operational factors, and geographic location significantly shape the energy yield and overall performance of photovoltaic (PV) systems. These variables have driven extensive research worldwide aimed at precisely quantifying and modeling PV output under diverse conditions to enhance understanding of their effects on system efficiency. It is well-documented that natural factors, especially solar radiation, play a significant role in causing fluctuations in power generation , as demonstrated by numerous studies, including Karami et al. (2017) [28], Al-Otaibi et al. (2015) [29], Layali Abu Hussein et al. (2021) [30] and Moafaq K.S. et al. (2022) [31].

Figure 10 offers a comparative evaluation of fixed and single-axis tracking subfields employing monocrystalline (mc-Si) and polycrystalline (pc-Si) technologies. Data collected at a 30° tilt angle includes ambient solar irradiance and cell irradiance, underscoring the significant influence of mounting configurations and tracking mechanisms on solar energy capture and system efficiency.

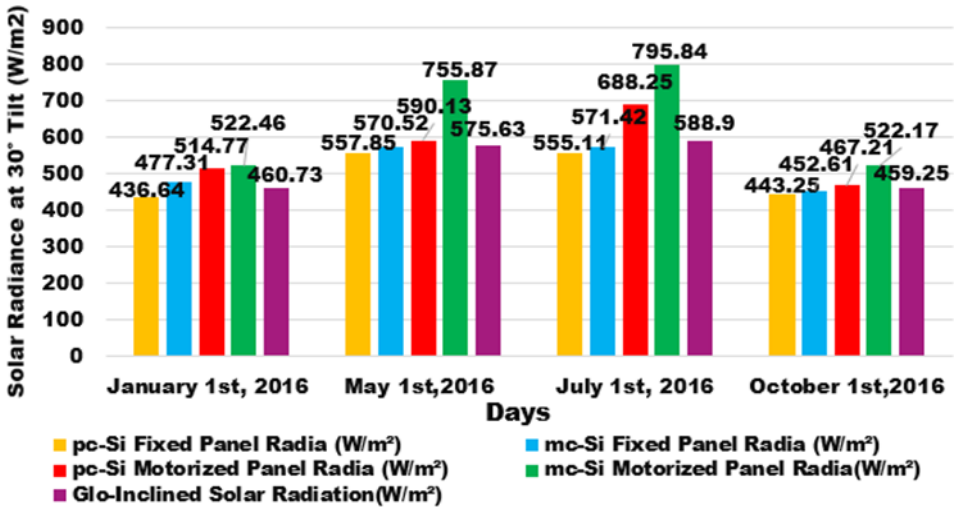

Fig 10. Seasonal Comparison of Inclined and Calibrated Cell Irradiance at 30° for Fixed and Tracking PV Subfields.

Seasonal comparison of inclined solar irradiance measured by a pyranometer and calibrated cell sensors positioned on each subfield at a 30° tilt, based on data from four experimental days in 2016 , as shown in Fig. 10.

On January 1st, a cold winter day with low solar altitude, the motorized mc-Si subfield recorded 522.46 W/m² about 9.5% higher than its fixed counterpart (477.31 W/m²). The motorized pc-Si performed even better, reaching 514.77 W/m² a 17.8% gain over the fixed version (436.64 W/m²). Both exceeded the ambient irradiance reference of 460.73 W/m², confirming the value of tracking under low-light conditions. On May 1st , under clear spring skies, the tracking advantage became more pronounced. The motorized mc-Si achieved 755.87 W/m², a 32.4% improvement over the fixed mc-Si (570.52 W/m²). Meanwhile, the motorized pc-Si showed a 5.8% gain (590.13 W/m² vs. 557.85 W/m²). Again, both values surpassed the ambient irradiance of 575.63 W/m². By July 1st , during the summer solstice and peak solar altitude, tracking systems delivered their highest performance. The motorized mc-Si registered 795.84 W/m², a 39.3% increase over the fixed mc-Si (571.42 W/m²), while the motorized pc-Si reached 688.25 W/m², outperforming the fixed version by 20.5%. Both readings exceeded the ambient value of 588.9 W/m². On October 1st , under mixed autumn sky conditions, tracking systems continued to show advantage. The motorized mc-Si reached 522.17 W/m² 15.4% higher than the fixed mc-Si (452.61 W/m²), while the motorized pc-Si improved by 5.4% (467.21 W/m² vs. 443.25 W/m²). Both remained above the ambient reference of 459.25 W/m².

Tracking systems improve solar irradiance capture throughout the year, with the most significant gains observed during periods of low and high solar altitude. They maintain optimal sun alignment on clear days and improve incidence angles under diffuse light conditions. While fixed subfields provide stable baseline performance, tracking configurations consistently outperform them. Monocrystalline (mc-Si) technologies absorb more irradiance than

Journal of Information Systems Engineering and Management
2025, 10(4)
e-ISSN: 2468-4376
https://www.jisem-journal.com/

Research Article

polycrystalline (pc-Si), emphasizing the importance of integrating high-efficiency PV modules with solar tracking to maximize annual performance.

X.2. Peak Power Generation and Daily Performance Analysis

Assessing the performance and power output of photovoltaic modules has been the focus of numerous studies across various regions, aiming to compare the efficiency and operational behavior of different PV technologies under diverse environmental conditions. A simulation study was conducted by Constance Kalu et al.(2019) [32] using PVsyst version 5.21, NASA meteorological data, and a hypothetical load demand. The study compares polycrystalline, monocrystalline, and thin-film photovoltaic (PV) technologies. The findings indicate that while thin-film PV technology offers low array loss, a low cost per unit of energy, and favorable performance metrics, it requires a larger installation area. Conversely, polycrystalline PV technology, with higher efficiency and smaller space requirements, is considered more suitable for the specific site due to its superior efficiency and compact design.

Additionally, Allouhi et al. (2016) [33] conducted a comprehensive assessment of 2 kWp grid-connected photovoltaic (PV) systems, both polycrystalline and monocrystalline silicon, installed at the High School of Technology in Meknes, Morocco, focusing on their performance, economic viability, and environmental impact. Nsengiyumva et al. (2018) [34] and Chien-Hsing et al. (2022) [35] found that solar tracking systems significantly increase energy capture compared to stationary systems. Further studies by Zaghba et al. (2018) [36] and Zaghba et al. (2019) [37] confirmed these findings. Vaziri Rad et al. (2020) [38] examined various tracking systems across different regions of Iran. They found that twin-axis trackers increased energy generation by 32%, while single-axis trackers resulted in a 23% increase compared to stationary systems. These findings underscore the critical role of tracking technology in improving the efficiency and overall performance of photovoltaic power plants.

A comparative study was conducted on two crystalline silicon photovoltaic (PV) technologies, monocrystalline silicon (mc-Si) and polycrystalline silicon (pc-Si), to assess the influence of different mounting configurations on power output optimization. Each technology was implemented using two types of support structures: a fixed-axis and a single-axis tracking system with an east–west orientation, both inclined at a 30° tilt angle. Each PV subfield had a rated capacity of 100 kWp. Real-time performance data were collected through field measurements conducted between 06:00 AM and 19:52 PM at four-minute intervals, as depicted in Figures 11–14. The evaluation focused on peak output power and long-term daily energy production across four representative dates in 2016 January 2nd , May 2nd , July 2nd , and October 2nd chosen to reflect seasonal climatic variations.

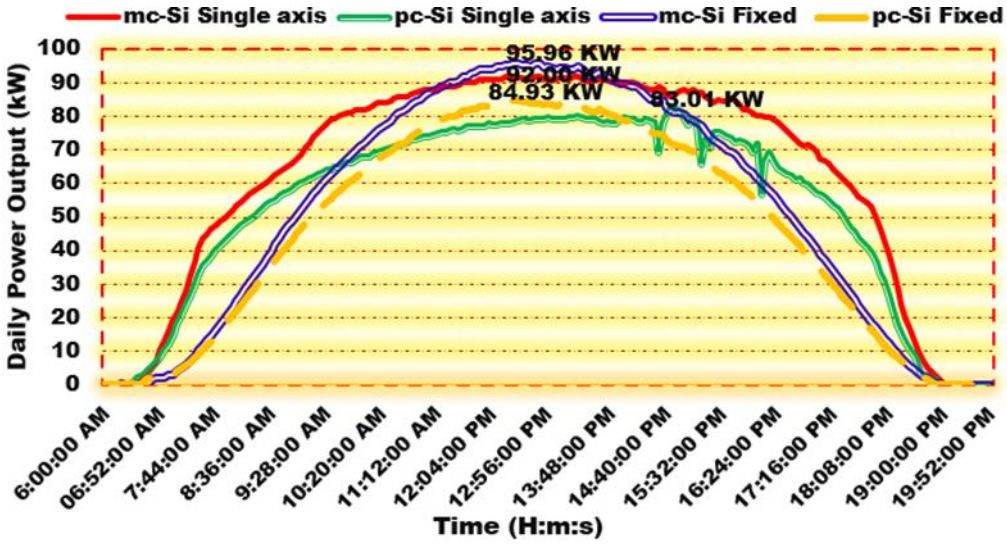

Fig. 11 illustrates the daily power output of mc-Si and pc-Si PV subfields using fixed and single-axis tracking configurations on January 2nd , 2016**.**

The highest peak output was recorded by the mc-Si fixed system, reaching approximately 89.99 kW at 12:56 PM. It was followed by the mc-Si single-axis system, which peaked at 80.77 kW at 12:04 PM, the pc-Si fixed system at 80.08

Journal of Information Systems Engineering and Management
2025, 10(4)
e-ISSN: 2468-4376
https://www.jisem-journal.com/

Research Article

kW at noon, and the pc-Si single-axis system, which recorded the lowest peak output of 73.98 kW at 11:20 AM. Although their peak values were lower, the single-axis systems produced more total daily power due to extended generation during morning and evening hours.

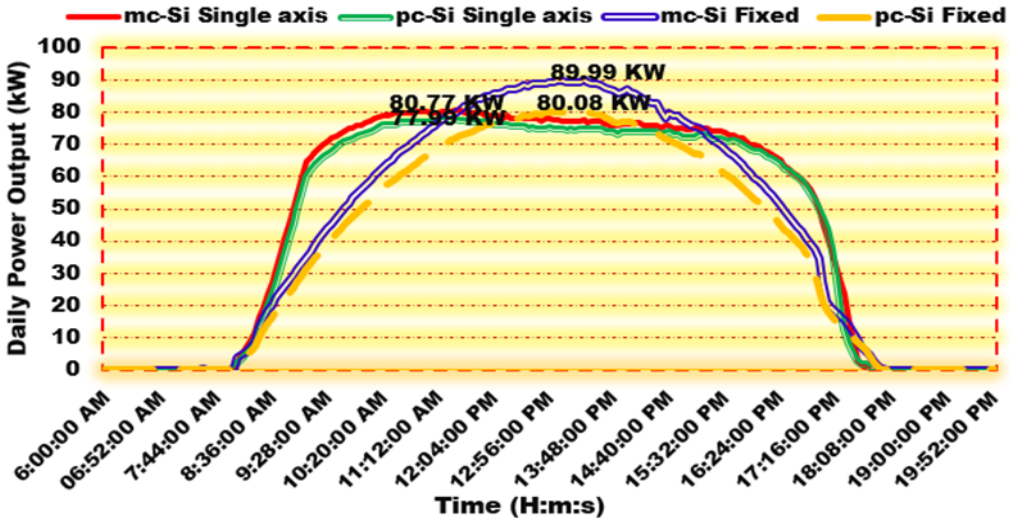

Fig 12. Comparison of Daily Power Generation from mc-Si and pc-Si PV Subfields Using Fixed and Single-Axis Tracking Systems on May 2nd , 2016 (Spring Conditions).

Figure 12 displays the variation in daily power output among four photovoltaic (PV) subfields, measured on May 2nd , 2016 a representative spring day. The highest peak output, 95.96 kW, was achieved by the mc-Si Fixed subfield at 12:23 PM. This was followed by the mc-Si Single Axis subfield, which reached a maximum of 92.20 kW at 12:20 PM. The pc-Si Fixed subfield recorded its peak of 84.93 kW at 12:56 PM, while the pc-Si Single Axis subfield achieved a maximum output of 83.01 kW at 2:40 PM. From this figure, it is evident that the mc-Si single-axis tracking system is the most effective in terms of both peak power output and total daily energy production **on** May 2nd . The implementation of tracking technology significantly enhances solar energy capture throughout the day, resulting in a higher overall power yield compared to fixed-mount configurations.

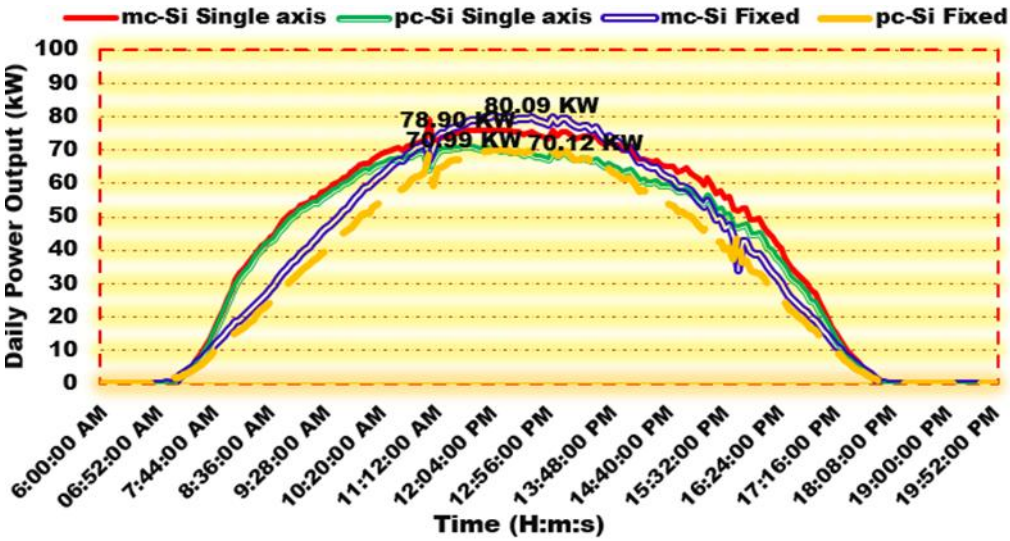

Fig 13. Comparison of Daily Power Generation from mc-Si and pc-Si PV Subfields Using Fixed and Single-Axis Tracking Systems on July 2nd , 2016 (Summer Conditions).

Journal of Information Systems Engineering and Management
2025, 10(4)
e-ISSN: 2468-4376
https://www.jisem-journal.com/

Research Article

Fig. 13. Shows the power output curves of four PV subfields on July 2nd , 2016, highlighting differences in performance between tracking and fixed configurations, notable differences in power output and system behavior, and compared to the previous day.

Among the subfields, the one-axis mc-Si system delivered the highest peak power, reaching 86.38 kW at 12:56 PM, followed by the fixed mc-Si subfield, which recorded 83.84 kW at 12:46 PM. The one-axis pc-Si subfield achieved 76.84 kW at 1:28 PM, while the fixed pc-Si configuration reached its peak of 71.12 kW. The results highlight the effectiveness of single-axis tracking systems, particularly when paired with high-efficiency mc-Si modules, which captured more solar radiation and delivered the highest power output. Although less significant, tracking also improved the performance of lower-efficiency pc-Si modules.

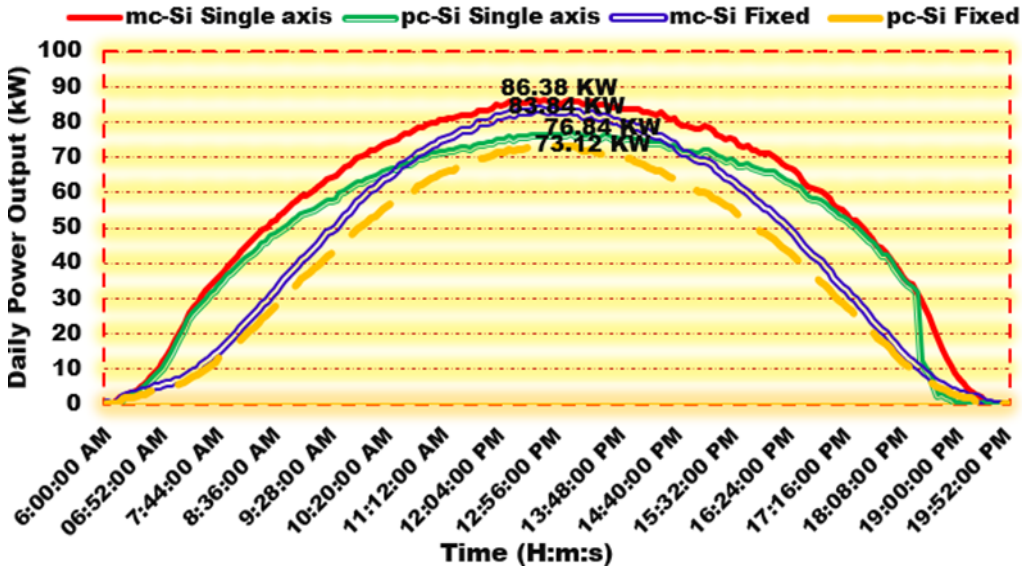

Fig14. Comparison of Daily Power Generation from mc-Si and pc-Si PV Subfields Using Fixed and Single-Axis Tracking Systems on October 2nd , 2016 (Full Conditions).

Figure 14 presents experimental data on the output power of fixed-axis and single-axis PV subfields recorded **on** October 2nd , 2016**,** a typical autumn day. The curves indicate that the fixed-axis mc-Si subfield delivered the highest output, reaching 80.09 kW at 12:28 PM. This was followed by the one-axis mc-Si subfield, which generated 78.90 kW at 11:25 AM. The one-axis pc-Si subfield achieved 70.99 kW at 10:55 AM, while the fixed pc-Si subfield produced a slightly lower peak of 70.12 kW at 1:08 PM. These results suggest that, under autumn conditions, the fixed mc-Si subfield outperformed its single-axis counterpart, indicating that high-efficiency modules can operate effectively without tracking in certain seasons.

- The experimental analysis conducted over four selected days demonstrates that the amount of DC power generated by photovoltaic panels is closely linked to their capacity to absorb solar irradiance. This capacity is significantly influenced by both the inclination angle and the use of solar tracking systems. Motorized tracking systems, particularly those with single-axis configurations, consistently enhance solar irradiance absorption by maintaining an optimal orientation toward the sun throughout the day. As a result, these systems achieve higher energy yields compared to fixed-tilt installations. The inclination angle further contributes by aligning the panel surface to maximize incident irradiance. Solar irradiance itself is identified as a critical factor in maximizing DC power output. These results are especially notable in the months of January 2nd, May 2nd, and July 2nd, where the single-axis tracking systems demonstrated a more consistent and elevated power output curve compared to fixed systems, underscoring the effectiveness of dynamic alignment in boosting overall energy production. This finding is consistent with those obtained by many authors who have studied solar tracking systems. Hafez et al. (2015) [39] and Layali Abu Hussein et al. (2021) [40].

Journal of Information Systems Engineering and Management
2025, 10(4)
e-ISSN: 2468-4376
https://www.jisem-journal.com/

Research Article

X.3 . Assessment of Daily and Average Power Generation.

This section presents a comparative analysis of average daily power generation (in kW) recorded over four representative days, based on experimental data. The analysis involves two photovoltaic technologies, monocrystalline silicon (mc-Si) and polycrystalline silicon (pc-Si), each mounted using single-axis tracking and fixed-tilt configurations, both inclined at 30°. The goal is to quantify the performance improvement provided by single-axis tracking systems. The results highlight the percentage increase (%) in power output relative to fixed systems. These findings are experimentally validated and presented in Figure 15 .

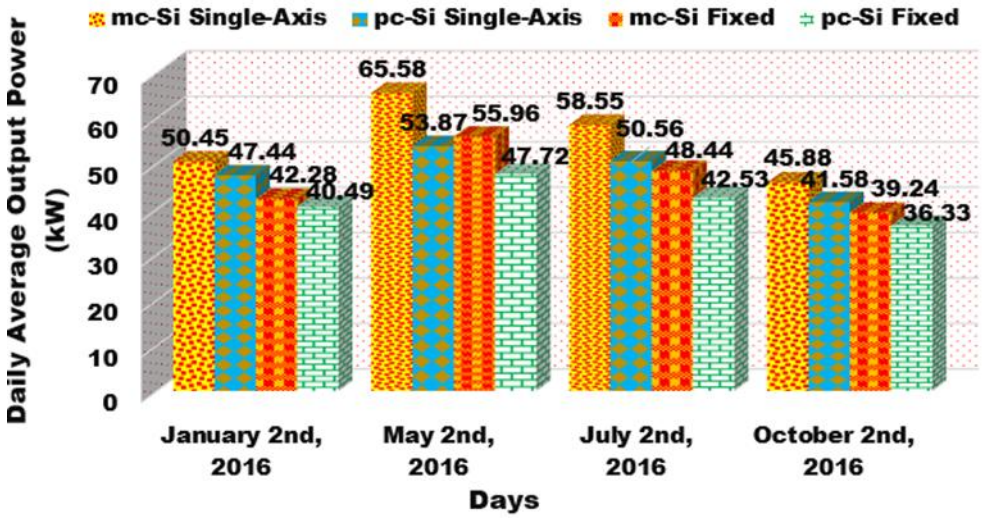

Fig 15 . Average Daily Power of Fixed and Single-Axis Tracking PV Subfields (mc-Si and pc-Si) Over Four Experimental Days .

Figure 15 illustrates the comparison of the average daily DC output power for multi-crystalline silicon (mc-Si) and polycrystalline silicon (pc-Si) technologies, analyzed under both fixed and single-axis tracking configurations across four experimental days, each representing a different season. The analysis also highlights the percentage increase in the tracking system's power output compared to the fixed configuration.

- On January 2nd , a typical winter day with low solar irradiance, the mc-Si single-axis tracking system achieved an average daily output of 50.45 kW. This surpassed the mc-Si fixed system, which produced 42.28 kW, resulting in an approximate increase of 19.3% in power generation due to the tracking mechanism. Similarly, the pc-Si single-axis tracking system recorded an average output of 47.44 kW, while the pc-Si fixed system generated 40.49 kW, indicating an increase of about 17.2%.
- On May 2nd , a spring day characterized by high solar radiation, the mc-Si single-axis tracking system achieved an average daily output of 65.58 kW. This performance surpassed that of the mc-Si fixed system, which generated 55.96 kW, marking an increase of approximately 17.2% due to the tracking mechanism. Similarly, the pc-Si single-axis system recorded an output of 53.87 kW, exceeding the pc-Si fixed system's output of 47.72 kW by about 12.9%. These results clearly demonstrate that single-axis tracking systems significantly enhance the power output of both mc-Si and pc-Si technologies, particularly under the high solar radiation conditions typical of spring. Notably, the mc-Si single-axis system exhibited a pronounced performance advantage over its fixed counterpart, highlighting the effectiveness of tracking systems in optimizing energy production during periods of favorable solar irradiance.
- On July 2nd under midsummer conditions with high solar irradiance, the mc-Si single-axis tracking system achieved an average daily output of 58.55 kW. This surpassed the mc-Si fixed system, which generated 50.56 kW, resulting in a performance gain of approximately 15.8% due to the tracking mechanism. Similarly, the pc-Si single-axis system produced 48.44 kW, exceeding the output of the pc-Si fixed system, which was 42.53 kW, by about 13.9%. These findings confirm the consistent performance advantages of single-axis tracking systems over fixed-tilt configurations, especially during the extended daylight hours and optimal solar angles characteristic of midsummer.

Journal of Information Systems Engineering and Management
2025, 10(4)
e-ISSN: 2468-4376
https://www.jisem-journal.com/

Research Article

➢ On October 2nd with the onset of autumn and a decline in solar irradiance, a decrease in output was observed across all systems. However, notable differences in performance between mounting configurations were still apparent. The mc-Si single-axis system generated 45.88 kW, surpassing the output of its fixed counterpart, which produced 39.24 kW an increase of approximately 16.9%. Similarly, the pc-Si single-axis configuration achieved an output of 41.58 kW, exceeding the pc-Si fixed system's output of 36.33 kW by about 14.4%.

CONCLUSION

This study presented a structured evaluation of four photovoltaic (PV) subfields incorporating monocrystalline (mc-Si) and polycrystalline (pc-Si) silicon technologies, deployed with either fixed-tilt or East–West oriented single-axis tracking systems. Each system was installed with a 30° tilt angle and designed for a peak capacity of 100 kWp. Performance analysis was carried out on four representative days across different seasons to assess how seasonal meteorological variations, particularly solar irradiance fluctuations, influence daily energy yields. The goal was to identify the most efficient system configuration under diverse climatic condition.

A detailed forecasting analysis of solar irradiance on a 30° inclined surface was conducted using three semi-empirical models: Perrin de Brichambaut, Liu & Jordan, and Capderou, utilizing real-time measured data. Among the three, the Perrin de Brichambaut model demonstrated the highest predictive accuracy, with correlation coefficients (CC) ranging from 0.9112 to 0.9985, and Root Mean Square Error (RMSE) values between 3.2261 W/m² and 7.3320 W/m². The Liu & Jordan model also showed good performance, with CC values from 0.8993 to 0.9888 and RMSE values ranging from 5.0293 W/m² to 8.2236 W/m². In contrast, the Capderou model had the lowest performance, with CC values ranging from 0.8812 to 0.9521 and RMSE values between 10.225 W/m² and 17.6434 W/m².

Evaluation of the Mean Absolute Percentage Error (MAPE) confirmed these findings. The Perrin de Brichambaut model exhibited the most stable error range (1.9684% to 8.869%), followed by Liu & Jordan (1.2236% to 11.251%). Capderou showed the widest variation (1.7855% to 21.225%), indicating lower reliability under variable conditions. Mean Absolute Error (MAE) results reflected similar trends: Perrin de Brichambaut showed the lowest MAE, ranging from 55.5830 W/m² to 101.2542 W/m²; Liu & Jordan ranged from 66.2512 W/m² to 152.336 W/m²; and Capderou from 88.6321 W/m² to 155.25 W/m². Additionally, the absolute error curve of Perrin de Brichambaut consistently remained close to the x-axis, indicating a strong agreement with measured values. While Liu & Jordan also provided good estimates, it showed more variability. Capderou was the least consistent, with notable daily deviations.

These findings confirm that the Perrin de Brichambaut model is the most reliable tool for predicting solar irradiance on a 30° inclined surface in Oued Nechou, Ghardaïa. Its high precision across multiple statistical metrics makes it particularly well-suited for Saharan contexts, especially where detailed meteorological station data may be lacking. This model thus constitutes a valuable asset for efficient solar energy planning in such environments.

Regarding PV system performance, the highest peak power values were observed on May 2nd The fixed mc-Si subfield recorded the maximum peak output at 95.96 kW, followed by the mc-Si single-axis tracker at 92 kW, the fixed pc-Si at 84.93 kW, and the pc-Si tracker at 83.01 kW. Despite the higher instantaneous power of fixed systems on this specific day, single-axis tracking configurations generally achieved higher total daily energy production due to their capacity to follow the sun's East–West path, thereby optimizing irradiance capture.

On May 2nd , the mc-Si tracking system generated an average of 65.85 kW per day, while the fixed mc-Si system produced 55.96 kW. Similarly, the pc-Si tracking system yielded 53.87 kW, which was an improvement over the 47.72 kW from the fixed pc-Si system. These outcomes correspond with the measured irradiance values. On May 2nd and July 2nd , the mc-Si tracking system received irradiance levels of 755.87 W/m² and 795.84 W/m², respectively, compared to 570.52 W/m² and 571.42 W/m² for the fixed mc-Si system. For the pc-Si systems, the tracking configuration captured 590.13 W/m² and 688.25 W/m², while the fixed configuration recorded 557.85 W/m² and 555.11 W/m².

The highest relative gains in energy production from tracking over fixed systems were observed on January 2nd and May 2nd . The mc-Si tracking system produced approximately 19.20% and 17.20% more power, respectively, than the

Research Article

fixed mc-Si configuration. The pc-Si tracker achieved gains of 17.20% on January 2nd and 14.40% on October 2nd compared to its fixed counterpart. The lowest gains were noted on July 2nd , with the mc-Si tracker exceeding the fixed system by 15.80%, and the pc-Si tracker showing a gain of 12.90% on May 2nd .

Overall, the mc-Si single-axis tracking subfield demonstrated the best performance in terms of energy gain and total power production. This confirms the suitability of combining monocrystalline technology with single-axis tracking for solar energy systems deployed in high-irradiance regions such as Oued Nechou and similar Saharan areas.

Future research should focus on optimizing technical configurations, managing maintenance in dusty environments such as Oued Nechou, and analyzing the long-term cost-effectiveness of tracking systems. The integration of additional performance criteria will enhance analyses and support the sustainable development of photovoltaic systems.

REFERENCES

[1] Benatiallah, A., Bouraiou, A., & Hamidat, A. (2017). Estimation of solar radiation in the Algerian Sahara using empirical models. Renewable and Sustainable Energy Reviews, 72, 343–355. https://doi.org/10.1016/j.rser.2017.01.040.
[2] Kalogirou, S. A. (2004). Solar thermal collectors and applications. Progress in Energy and Combustion Science, 30(3), 231–295. https://doi.org/10.1016/j.pecs.2004.02.001 .
[3] B . Marion, B. Smith, “Photovoltaic system derived data for determining the solar resource and for modeling the performance of other photovoltaic systems,” Sol. Ener., vol. 147, no. 2, pp. 147–357, May. 2017.
[4] A. Gougui, A. Djafour, N. Khelfaoui and H. Boutelli, “Empirical models validation to estimate global solar irradiance on a horizontal plan in Ouargla, Algeria,” presented In AIP. Conf. Proceedings, May, 2018.
[5] V. Sharma, S. S. Chandel, “Performance analysis of a 190 kWp grid interactive solar photovoltaic power plant in India,” Energ., vol. 55, pp. 476–485, Jun. 2013.
[6] M. E. H. Dahmoun, B. Bekkouche, K. Sudhakar, M. Guezgouz, A. Chenafi, A. Chaouch, “Performance evaluation and analysis of gridtied large scale PV plant in Algeria,” Ene. for. Sus. Devel., vol. 61, pp. 181–195, Apr. 2021.
[7] S.B. S. Kumar, K. Sudhakar, “Performance evaluation of 10 MW grid connected solar photovoltaic power plant in India,” Ene. repo., vol. 1, no. 2, pp. 184–192, Nev. 2015.
[8] S. Touili, A. Alami Merrouni, Y. El Hassouani, A. I. Amrani, “Performance analysis of large scale grid connected PV plants in the MENA Region,” Int. J. of. Eng. Res. in. Afri., vol. 42, pp. 139–148, Apr. 2019.
[9] Y. El Mghouchi , A. El Bouardi, Z. Choulli, T. Ajzoul , “ Models for obtaining the daily direct, diffuse and global solar radiations,”, Renewable and Sustainable Energy Reviews 56 (2016) 87–99 .
[10] M. R. Yaïche, S. M. A Bekkouche, “Estimation du rayonnement solaire global en Algérie pour différents types de ciel,” Revue des Energies Renouvelables. Renewable Energies. J. Vol. 13, pp.683-695, Decembrev 2010.
[11] Cooper PI. The absorption of radiation in solar stills. Solar Energy 1969;12:333–46 Pergamon Press.
[12] Y. El Mghouchi, A. El Bouardi, Z. Choulli, T. Ajzoul, “Models for obtaining the daily direct, diffuse and global solar radiations,” Elsevier. J. Renewable and Sustainable Energy Reviews, Vol.56, pp.87-99, April 2016.
[13] A. Bensaha, F. Benkouider, S. M. A. Bekkouche, “Estimation du rayonnement solaire en ciel clair par des modèles empiriques : Application au site de Ghardaïa Algérie,” 1st International Seminar on The Apport of The Simulation in Technological Innovation, pp. 1-5, November 2016
[14] Bouramdane Abderraouf , Louazen Mohamed Lakhdar, Benmir Abdelkader , " Forecasting global incline solar radiation through empirical models on Desert areas " , Fourth International Conference on Technological Advances in Electrical Engineering (ICTAEE’23.), pp-1-8 , May 23-24 2023 .
[15] M. Ghodbane, B. Boumeddane, “Estimating solar radiation according to semi empirical approach of PERRIN DE BRICHAMBAUT: application on several areas with different climate in Algeria,”International Journal of Energetica. J, vol. 1, pp. 20–29, December 2016.
[16] GOUGUI Abdelmoumen , « Étude et expérimentation d’un système hybride photovoltaïque/hydrogène pour l’intégration dans le système électrique», Thèse de doctorat, université de Ouargla . 2021.
[17] M. Louazine, « Étude technico-économique d'un système de pompage photovoltaïque sur le site de Ouargla », Mémoire de Magister de l’université de Batna 2008.

Research Article

[18] Liu, B.Y.H.; Jordan, R.C. “Daily insulation on surfaces tilted towards the equator”, Trans. ASHRAE, 1962, 53, 526-41.
[19] A. Moummi, N. Hamani, N. Moummi & Z. Mokhtari, “Estimation du rayonnement solaire par deux approches semi empiriques dans le site de Biskra,”8ème Séminaire International sur la Physique Energétique. Algérie, pp. 1–6, Novembre 2006 .
[20] A. M. M. H. e. A. G. F.Yettou, " Etude comparative de deux modèles de calcul du rayonnement solaire par ciel clair en Algérie ", Revue des Energies Renouvelables , vol. Vol. 12 N°2, n° %1331 – 346, 2009.
[21] M.HAMDANI, « Étude et Effet de l’Orientation de deux Pièces d’un Habitat en Pierre Situé à Ghardaïa », Thèse de doctorat, université de Ghardaïa, 2011.
[22] M.CAPDEROUX, Atlas Solar on l’Algérie Modèles théoriques et expérimentaux.tome1.Vol. 1. 2. Office des publications Universitaires: Alger 1987.
[23] H. Duzen, H. Aydin, “ Sunshine-based estimation of global solar radiation on horizontal surface at Lake Van region (Turkey),” Elsevier. J. Energy Conversion and Management, vol. 58, pp. 35–46, June 2012.
[24] M. Koussa, A. Malek, M. Haddadi, “Statistical comparison of monthly mean hourly and daily diffuse and global solar irradiation models and a Simulink program development for various Algerian climates,”Elsevier. J. Energy Conversion and Management, vol. 50, pp. 1227–1235, May 2009.
[25] M. M. Khanand M. J. Ahmad, “Estimation of global solar radiation using clear sky radiation in Yemen,” Journal of Engineering Science and Technology Review. J, vol. 5, pp. 12–19, August 2012.
[26] H, Li, X, Bu , Z, Long , L, Zhao, W, Ma, “ Calculating the diffuse solar radiation in regions without solar radiation measurements,”Elsevier. J. Energy, vol. 44, pp. 611–615, August 2012.
[27] T. E. Boukelia, M. S. Mecibah, I. E. Meriche, “General models for estimation of the monthly mean daily diffuse solar radiation (Case study: Algeria),”Elsevier. .J . Energy Conversion and Management, Vol.81,pp. 211-219, May 2014.
[28] E. Karami, M. Rafi, A. Haibaoui, A. Ridah, B. Hartiti and P. Thevenin, “Performance analysis and comparison of different photovoltaic modules technologies under different climatic conditions in Casablanca,” Jou. of. Fun.of. Ren.Ene.and.Appli., vol. 7, no. 3, pp. 1–6, 2017.
[29] Al-Otaibi, A. Al-Qattan, F. Fairouz, A. Al-Mulla, “Performance evaluation of photovoltaic systems on Kuwaiti schools’ rooftop,” Ene. Con.and. Mana., vol. 95, pp. 110–119, May. 2015.
[30] L. A. Hussein, O. Ayadi and M. Fathi, “Performance comparison for sun-tracking mechanism photovoltaic (PV) and concentrated photovoltaic (CPV) solar panels with fixed system PV panels in Jordan,” presented at the 12th Int. renewable engineering. Conf. IEEE , Amman, Jordan, Apr, 2021.
[31] M. K. Al-Ghezi, R. T. Ahmed, M. T. Chaichan, “The Influence of Temperature and Irradiance on Performance of the photovoltaic panel in the Middle of Iraq,” Int. Jou. of. Ren. Ene. Deve., vol. 11, no. 2, pp. 501–513, 2022.
[32] C. Kalu, I. A. Ezenugu, A. M. Umoren, “Comparative study of performance of three different photovoltaic technologies,” Mat. and. Sof. Engi., vol. 2, no. 1, pp. 19–29, 2019.
[33] A . Allouhi, R. Saadani, T. Kousksou, R. Saidur, A. Jamil, M. Rahmoune, “ Grid-connected PV systems installed on institutional buildings: Technology comparison, energy analysis and economic performance,” Ene. and. Buil., vol. 130, pp. 188–201, Oct. 2016.
[34] W . Nsengiyumva, S. Chen, L. Hu, X. Chen, “Recent advancements and challenges in Solar Tracking Systems (STS): A review,” Ren. and Sus. Ene. Revie., vol. 81, pp. 250–279, Jan. 2018.
[35] C.H. Wu, H. C. Wang, H. Y. Chang, “Dual-axis solar tracker with satellite compass and inclinometer for automatic positioning and tracking,” Ene. for. Sus. Devel., vol. 66, pp. 308–318, Feb. 2022.
[36] L. Zaghba, M. Khennane, A. Borni, A. Fezzani, I. Hadj Mahammed and A. Bouchakour, “Intelligent MPPT Control of Stationary and Dual-axis Tracking Grid-connected Photovoltaic System,” SCI. Dig. Libra., vol. 1, pp. 199–205, 2018.
[37] L. Zaghba, M. Khennane, A. Fezzani, A. Borni and I. H. Mahammed, “Experimental outdoor performance evaluation of photovoltaic plant in a Sahara environment (Algerian desert),” Int. J. of Amb. Ener., vol. 43, no. 1, pp. 314–324, Jul. 2019.
[38] M. A. Vaziri Rad, A. oopshekan, P. Rahdan, A. Kasaeian, O. Mahian, “A comprehensive study of techno-economic and environmental features of different solar tracking systems for residential photovoltaic installations,” Ren. and. Sus. Ene. Revi., vol. 192, 2020.

Journal of Information Systems Engineering and Management
2025, 10(4)
e-ISSN: 2468-4376
https://www.jisem-journal.com/

Research Article

[39] A. Z. Hafez, J. H. Shazly and M. B. Eteiba, "Comparative evaluation of optimal energy efficiency designs for solar tracking systems," presented .In Proc.Of the third intl. Conf. on advances in applied science and environmental engineering, Apr. 134-141, 2015.

[40] L. A. Hussein, O. Ayadi and M. Fathi, "Performance comparison for sun-tracking mechanism photovoltaic (PV) and concentrated photovoltaic (CPV) solar panels with fixed system PV panels in Jordan," presented at the 12th Int. renewable engineering. Conf. IEEE , Amman, Jordan, Apr, 2021